Bibliographical reference

Reflection at the Cut-off and Transmission by Tunnel Effect in a Waveguide with Linear Section Variation, Z. Hamitouche, M. Ech-Cherif El-Kettani, J.-L. Izbicki and H. Djelouah, Acta Acustica **vol. 95** (Number 5), 2009, pp. 789-794

DOI

https://doi.org/10.3813/AAA.918209

Acta Acustica united with Acustica
Vol. 95 (2009) 789 – 794

Scientific Papers
DOI 10.3813/AAA.918209

Reflection at the Cut-off and Transmission by Tunnel Effect in a Waveguide with Linear Section Variation

Z. Hamitouche, M. Ech-Cherif El-Kettani, J.-L. Izbicki
Laboratoire Ondes et Milieux Complexes LOMC FRE CNRS 3102, University of Le Havre, IUT of Le Havre, Place Robert Schuman, 76610 Le Havre, France. elkettani@univ-lehavre.fr

H. Djelouah
Laboratoire de Physique des Materiaux, Faculty of Physics, University of Algiers, Algiers, Algeria

Summary
We present experimental and numerical results on the propagation of Lamb waves in duraluminum elastic waveguides whose section is varying linearly from 5 mm to 2 mm. The Lamb mode is generated in the area of 5 mm thickness and is propagating down slope. If the incident Lamb wave propagating down slope reaches its thickness cut-off in the varying section area, it is totally reflected. However, a small part of its energy is transmitted by tunnel effect to the area of 2 mm thickness, and is converted into other Lamb waves. The tunnel length and the energy distribution on the transmitted waves are given as function of frequency. Experimental and numerical results are in good agreements.

PACS no. 43.20.El, 43.20.Mv, 43.20.Ye, 43.35.Cg, 43.35.Pt, 43.40.Fz

1. Introduction

The propagation of Lamb waves in a plate with a constant section is well known analytically and experimentally. The case where the waveguides include a varying section zone remains a problem. Most previous works on these topics are theoretical and predict the existence of adiabatic waves in the case of slow and continuous section variation, as well as modes conversion [1, 2, 3, 4, 5, 6]. These predictions have been confirmed by experimental and numerical works [7, 8, 9, 10]. Numerical approaches were developed such as hybrid boundary-element methods [11, 12], finite-element methods [13, 14] and modal methods [15, 16]. In the case of waveguides with linearly varying section, previous experimental and numerical works have shown the reflection of the propagating guided wave when reaching its thickness cut-off [7]. The aim of this work is to study the propagation in plane plates including an area whose section is linearly varying from 5 mm to 2 mm thickness. The A_1 Lamb mode will be generated in the thicker area. Its propagation down slope inside the varying section domain and its transmission into the thinner area will be on the focus. Its adiabatic behaviour and its total reflection into the same mode when it reaches its thickness cut-off (located before the end of the varying section domain) are expected and will be shown. But more interesting is to show, even if this mode is totally reflected, that a small part of its energy is transmitted to the thinner zone giving rise to propagating Lamb modes. The transmitted energy is evaluated and compared to the one carried by the incident A_1 mode.

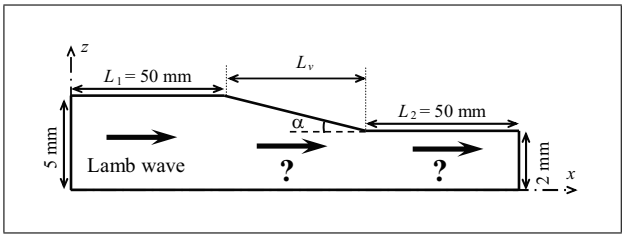

Figure 1. Waveguides geometry.

The studied waveguides are in duraluminum with longitudinal wave velocity $C_L = 6380$ m/s, shear wave velocity $C_T = 3100$ m/s and density $\rho = 2800$ kg/m^3. Figure 1 gives the geometrical shape of the waveguides. The waveguides are only differing by the slope angle of their varying section domain: $\alpha = \arctan(\Delta d(\text{mm})/L_v(\text{mm}))$, with $alpha = 8.5°$ ($L_v = 20$ mm), $\alpha = 5.7°$ ($L_v = 30$ mm) and $\alpha = 4.3°$ ($L_v = 40$ mm).

In the next section a short description is given for experimental and numerical methods [8, 10], the signal processing is also presented before the analysis of results.

Received 25 June 2008,
accepted 6 April 2009.

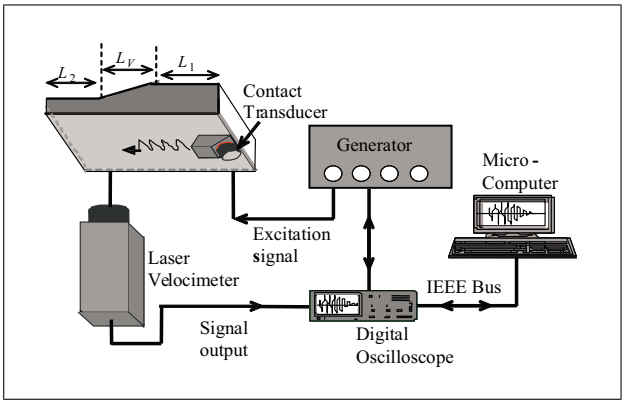

Figure 2. Experimental set-up.

2. Experimental study

Figure 2 shows the experimental device. The excitation of the Lamb wave is carried out with a contact transducer of 1 MHz central frequency (useful bandwidth extends from 0.5 MHz to 1.5 MHz), fixed on a Plexiglas wedge of 26 degrees geometrical angle. This value is chosen in order to generate the A_1 mode which has a cut-off of 1.55 MHz mm. The excitation signal is quasi-harmonic of 0.66 MHz central frequency with ten cycles duration, weighted with a gaussian waveform of 10 Vpp maximum amplitude. This central frequency is chosen because during the down slope propagation, the A_1 mode will reach its thickness cut-off $d_{\text{cut}} = 2.35$ mm. A laser velocimeter measures the normal displacement versus time on the plate flat surface in the propagation direction and is translated by steps of 0.2 mm over 150 mm. The signal is acquired over 100 µs duration and is sampled at 100 MHz by a digital oscilloscope. The measurements are recorded on a microcomputer and arranged in a time-space matrix.

3. Numerical study

The numerical study is based on the Finite Elements Method (FEM), developed in 2-D, using the Comsol software in transient analysis.

A quadratic meshing with isoparametric nodes is used. The normal U_Z and tangential U_X components of the theoretical displacements of the chosen A_1 Lamb wave are applied on the nodes of the thicker section (5 mm thickness), during ten periods.

For the numerical study, the temporal Δt and the spatial Δx steps must be chosen in order to obtain a good convergence of the numerical solution [17]. For the spatial meshing of the domain, a minimum of five meshes per wavelength is commonly required. In our case, the spatial step is the same as that in the experiment where $\Delta x = 0.2$ mm is used, allowing approximately 42 steps per wavelength. The temporal step is $\Delta t = 1/22f$, which is enough for a correct time sampling. The normal displacements of the nodes on the flat side are collected as in experiment, and processed in the same way.

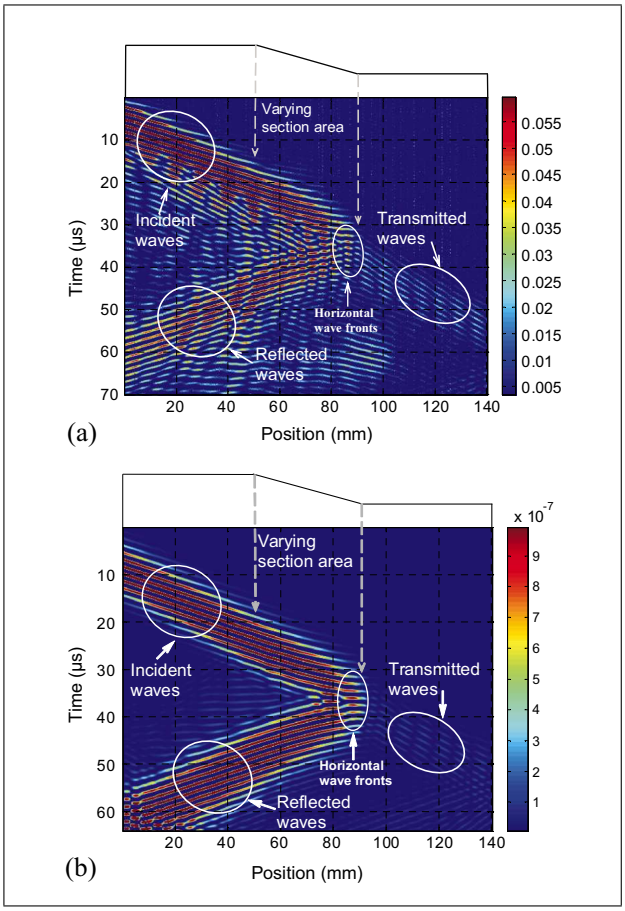

Figure 3. Time-position representation, waveguide with $\alpha = 4.3°$, A_1 incident mode, f = 0.66 MHz. a: Experimental study. b: Numerical study.

4. Signal processing

The signal processing performed in this study has often been used in other works, and is therefore well tested [7, 8, 9, 10]. It is just summarized in the following. Space-time FFT is performed for modes identification, and gives a wavenumber versus frequency representation. For each position the recorded signal is extended to 16384 points by a zero padding technique. The accuracy on the value of the wavenumber is $dk = 3.83$/m and on the value of the frequency is $df = 1.74$ kHz. In order to follow the propagation of the Lamb wave, the wavenumber versus position representation is also obtained with spatial FFT by sliding a Gaussian window at a fixed frequency. The size of the sliding window, which results from a compromise between precision on the position and on the wavenumber, is fixed to 40 mm. This processing gives an accuracy of $dk = 1.92$/m on the wavenumber. This representation is particularly well suited to our case because the observation and the characterization of the wave propagation along the waveguide are of interest.

5. Experimental and numerical results

The wedge angle of 26 degrees and the incident beam have been arranged in order to generate experimentally the A_1

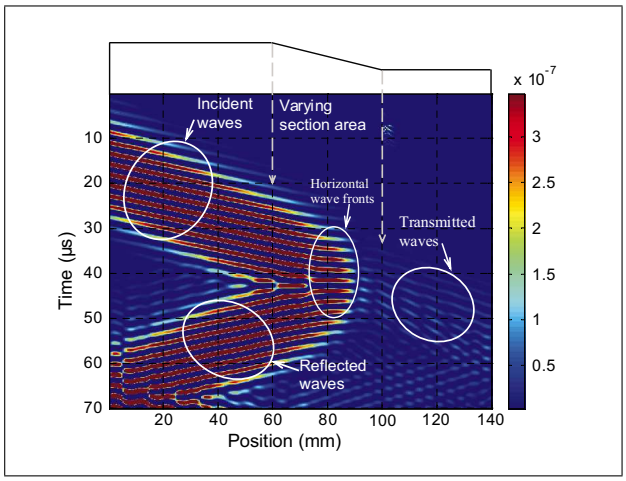

Figure 4. Numerical study: Time-position representation, waveguide with $\alpha = 4.3°$, A_1 incident mode, $f = 0.42$ MHz.

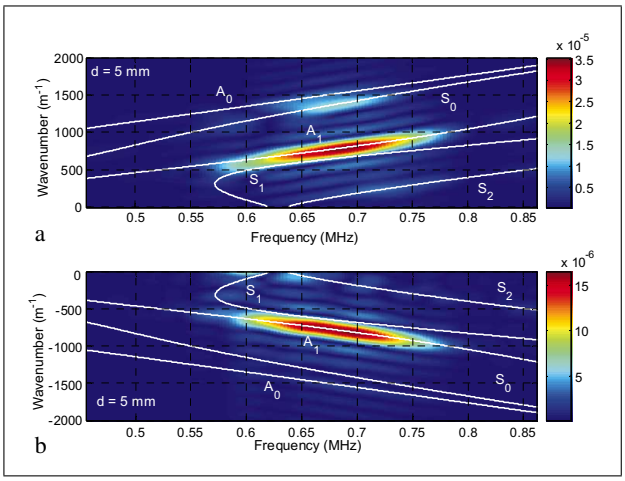

Figure 5. Experimental study: Wavenumber versus frequency representation in the area of 5 mm thickness. Waveguide with $\alpha = 4.3°$. a: Incident A_1 mode, b: Reflected A_1 mode.

mode in the thicker area. The central frequency of the signal is 0.66 MHz. The plots with colour levels of the time-position matrix, for both experimental and numerical studies, are given on Figure 3a and 3b. The incident, reflected and transmitted signal represented by the magnitude of the normal displacement are shown in (x, t) diagram. One can observe the propagation of waves that are mainly reflected before reaching the end of the varying section domain. A small part is transmitted in the area of 2 mm thickness. Figure 3a corresponding to the experimental study contains more wave fronts compared to Figure 3b corresponding to the numerical one. This is due to multiple reflections within the wedge that generate supplementary wave fronts.

It is important to note that at $f = 0.66$ MHz, the thickness cut-off in the varying section area of the A_1 mode is equal to 2.35 mm, which is very close to the area of 2 mm thickness. Nevertheless, one can see that the wave fronts become horizontal, indicating an infinite velocity: this is a characteristic of the wave at its cut-off. To confirm this reflection at the cut-off before reaching the end of the varying section domain, another simulation is then carried at a lower frequency. Figure 4 is a time-space representation of the incident A_1 mode generated at $f = 0.42$ MHz. One can clearly observe its reflection before the end of the varying section domain. Here again, when it reaches its thickness cut-off, a small part of the energy is transmitted in the area of 2 mm thickness.

In the following, some results will be given for experimental and numerical studies, for the A_1 incident mode at $f = 0.66$ MHz, as the transducer bandwidth does not permit any study at $f = 0.42$ MHz.

5.1. Modes identification in the thicker area

A space-time FFT is applied in the area of 5 mm thickness. Figure 5a and 5b show the wavenumber versus frequency representation for experimental data. Figure 5a corresponding to positive values of wavenumbers is related to the generated incident modes. Theoretical dispersion curves of Lamb modes are superimposed. The A_1

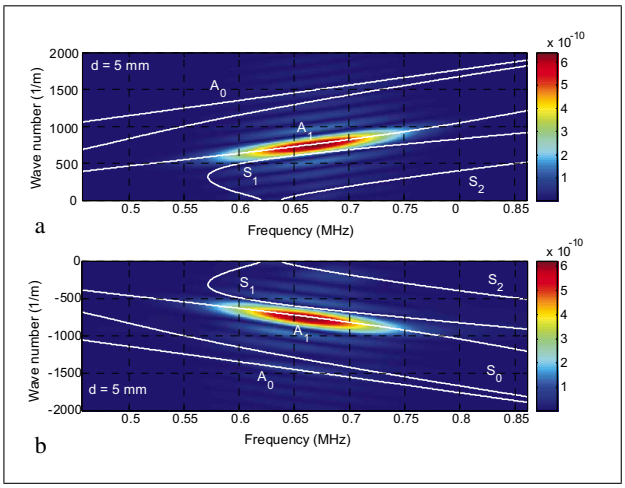

Figure 6. Numerical study: Wavenumber versus frequency representation in the area of 5 mm thickness. Waveguide with $\alpha = 4.3°$. a: Incident A_1 mode, b: Reflected A_1 mode.

mode is identified in the frequency range 0.57 MHz $< f <$ 0.77 MHz. In addition, the S_0 mode is also weakly generated around the central frequency of excitation. Figure 5b, with negative wavenumber values, is related to the reflected A_1 mode propagating backward. One can see that this mode is reflected in all the frequency range of excitation. Figure 6a and 6b are the same representations for the numerical study. A very good agreement can be seen between the experimental and numerical results. In spite of the phenomenon of total reflection, the amplitude of the reflected wave observed in experiment is smaller than the one of the incident wave. This is due to the geometrical spreading of the beam on the plate. Such a phenomenon is not seen in the numerical studies because a pure 2D problem is solved by the numerical scheme.

For all the frequencies existing in the spectrum of the incident A_1 mode, there is a critical thickness in the varying section. The frequency-thickness cut-off for the A_1 mode is 1.55 MHz mm. For the lowest frequency of excitation,

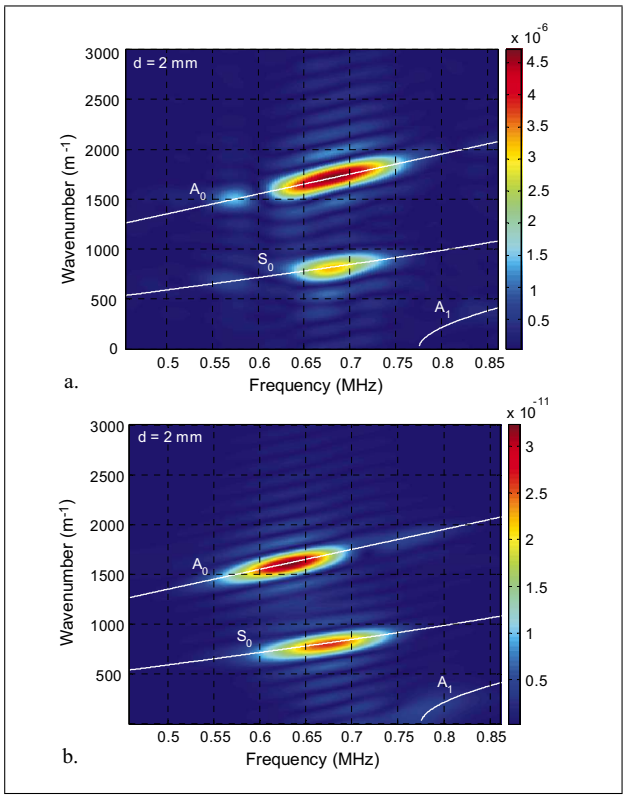

Figure 7. Wavenumber versus frequency representation in the area of 2 mm thickness. Waveguide with $\alpha = 4.3°$. a: Experimental study, b: Numerical study.

the thickness cut-off is $d_{\text{cut}} = 1.55/0.57 = 2.72\,\text{mm}$, and for the highest $d_{\text{cut}} = 1.55/0.77 = 2.01\,\text{mm}$, that are both included in the varying section domain. Then it can be considered that the entire A_1 wave is retro-reflected. The analysis of the thinner zone will show if any acoustic field is however transmitted.

5.2. Transmitted modes and their energy

The modes identification process is achieved on experimental and numerical data in the transmission zone. Figure 7a and 7b show the wavenumber-frequency representation in the area of 2 mm thickness, respectively for the experimental and numerical study. The transmitted A_0 and S_0 modes are identified, in both cases. The A_0 mode seems to be transmitted in a wider frequency range. The amplitude distribution of these modes in the experiment is slightly different from the simulation, which could result from the excitation of the incident S_0 mode in addition to the A_1 (previous studies have shown that the incident S_0 mode gives rise to the S_0 and A_0 transmitted modes in the thinner area). Therefore, the energy distribution of the incident A_1 mode on the transmitted modes will be only calculated for the numerical study.

Experimentally, the process to determine the energy of a Lamb mode from its normal displacement is currently used in our previous works [9, 10]. For a waveguide of constant thickness, a theoretical coefficient is calculated: $\zeta = |U_z|/\sqrt{\phi}$, where U_z is the normal displacement and ϕ

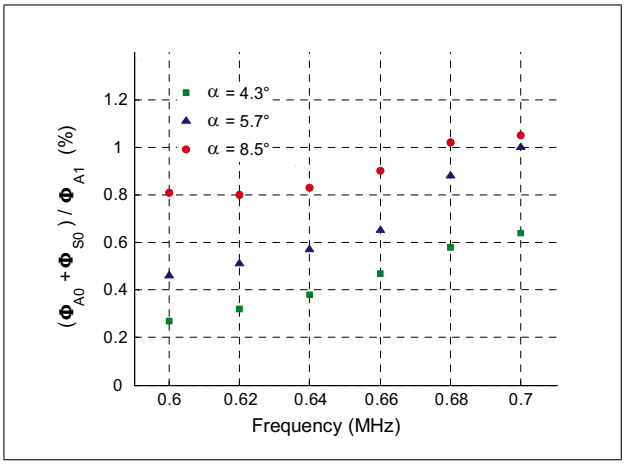

Figure 8. Numerical study: Ratio of the total transmitted energy by the incident one versus frequency.

the energy of the considered mode (the energy is defined as the Poynting vector flow in the propagation direction across the section of a plane elastic plate) [18]. The knowledge of the ζ parameter and the measure of the normal displacement obtained for the considered structure from the experiment or the FEM, gives the value of the energy. Numerically, an energy balance is made in the thick and the thin zones. It is possible to get the energy of the incident and reflected waves at the thicker area and the transmitted energy at the thinner area. The law of conservation of energy is verified within an error of about 2%. Cuts at different frequencies on the wavenumber-frequency representation are done [9, 10], and the ratio of the total energy carried by the transmitted modes by the energy of the incident A_1 mode $(\phi_{S_0} + \phi_{A_0})/\phi_{A_1}$ is calculated. Figure 8 is the plot of this ratio versus frequency for different waveguides whose sections are varying from 5 mm to 2 mm, but with different slopes.

The various curves exhibit a similar evolution. The total transmitted energy is very small compared to the incident one, and does not exceed 1.2%. Moreover, the total transmitted energy at a given frequency is more important when the slope of the guide increases. Interpretation of the physical phenomenon that allowed this transmission is given in section 5.4. The adiabatic behaviour of the incident A_1 mode is on the focus in the next section.

5.3. Adiabatic behaviour inside the varying section domain

Figures 9a and 9b are the representation of the wavenumber versus position using a spatial FFT with sliding window at $f = 0.66\,\text{MHz}$, obtained respectively for the experiment and the simulation. The colour levels indicate the value of the modulus of the FFT. The guide profile is also drawn on the right side of these figures to locate the positions where the propagating wave exhibits some particular properties. The positive values of wavenumbers indicate propagation towards the decreasing thickness, while negative the opposite. The dispersion curves of Lamb waves

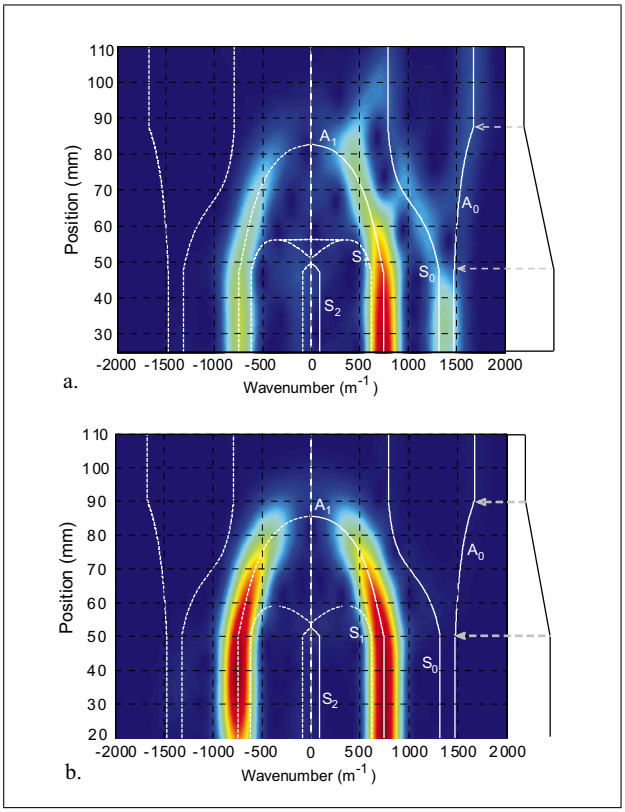

Figure 9. Wavenumber versus position representation using spatial FFT with sliding window at $f = 0.66$ MHz. Waveguide with $\alpha = 4.3°$. a: Experimental study, b: Numerical study.

for the local thickness and at $f = 0.66$ MHz are also plotted. These figures confirm the well-expected adiabatic behaviour of the incident A_1 mode inside the varying section domain [6, 7, 8, 9], but more interesting is its reflection at a particular thickness $d = d_{\text{cut}}$ corresponding to the cut-off of the A_1 Lamb mode at the considered frequency. The propagation of this mode is then upslope. Two modes A_0 and S_0 are weakly transmitted in the area of 2 mm thickness, as shown in section 5.2. As the S_0 mode is generated in addition to the A_1 mode in the experiment (see Figure 9a near 1300/m), the origin of these transmitted waves is not so clear. The numerical study brings the physical meaning of the propagation of waves in the transmitted area, because the transmission is only related to the incidence of the A_1 mode in the numerical study (Figure 9b).

5.4. Interpretation

Propagating Lamb modes are real solutions of the characteristic equation of a plate for frequencies higher than their cut-off. Below this cut-off, the solutions are complex or purely imaginary and are related to an evanescent field. In the area beyond the limit $d = d_{\text{cut}}$, an evanescent field can exist. This fact is related to the evolution of the wave vector in the complex plane. As the A_1 wave is propagating, the wavenumber is real, that is $K_x = K'_x(\omega d)$. At the frequency-thickness cut-off: $K'_x = 0$. Below this cut-off, the wavenumber in the case of the A_1 mode, is purely imaginary: $K_x = \mathrm{i}K''_x$. The dispersion curve of the

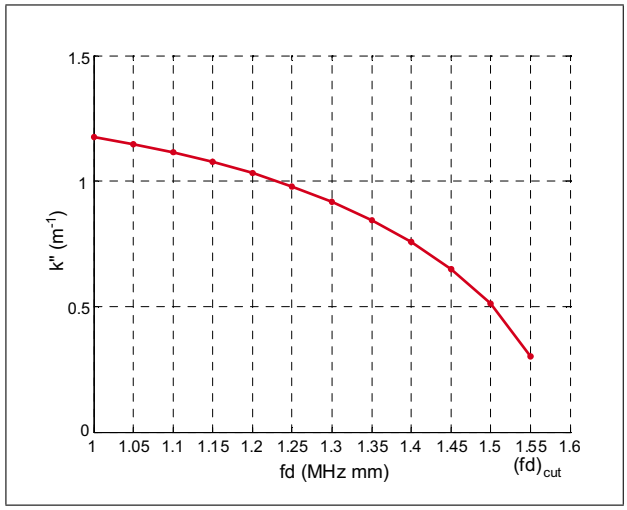

Figure 10. Dispersion curve of the evanescent A_1 Lamb Mode.

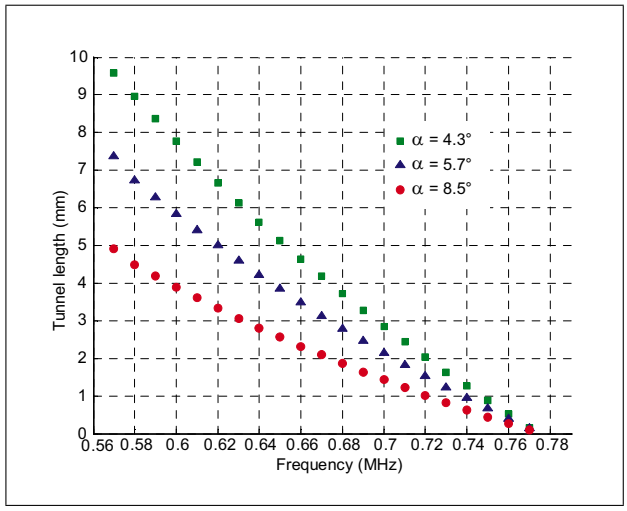

Figure 11. Numerical study: Variation of the tunnel length versus the frequency for the different studied guides.

evanescent A_1 mode is shown on Figure 10. The imaginary wavenumber is increasing when the frequency-thickness is decreasing, that is the amplitude of the vibration for $d < d_{\text{cut}}$ is decreasing. Nevertheless for a length with an order of magnitude equal to $1/K''_x$, the amplitude is weak but not null. It can be considered that the vibrations located at the beginning of the zone of constant thickness give rise to waves that can propagate at the considered frequency. In this case for the thickness and the frequency considered, only two waves can propagate: A_0 and S_0 waves. Their transmission is then assumed to be by tunnel effect. This phenomenon of guided wave tunnelling is rather classical of theoretical physics encountered in many fields, and has been reported by A. Alippi *et al.* for example, in the case of the backward propagating S_1 Lamb mode [19].

The distance between the position of the thickness cut-off d_{cut} and the entry of the transmission area appears to be a tunnel length. These tunnel lengths are given on Figure 11 as a function of frequency. For a given waveguide, when the frequency increases, the thickness cut-off de-

creases, that is the tunnel length decreases, and the transmitted energy increases (see Figure 8), which is in agreement with the tunnel effect. In another hand, Figure 10 shows that the imaginary wavenumber is increasing as the frequency-thickness is decreasing, that means as the tunnel length is increasing. Therefore, the transmitted energy must be decreasing: this fact is in accordance with the measured transmitted energy and confirms the tunnel effect transmission.

At a fixed frequency, the transmitted energy is more important when the slope of the waveguide increases as the tunnel length becomes shorter. Figures 8 and 11 confirm these points of view and support the mode transmission by tunnel effect.

6. Conclusion

In this work we have shown experimentally and numerically the reflection of an incident Lamb mode when it reaches its thickness cut-off in a waveguide including a linear section variation. The experimental and numerical results are in good agreement. The numerical study helps to highlight the physical meaning of the observed phenomenon. A small part of the incident mode energy is transmitted by tunnel effect into Lamb modes in the thinner part of the waveguide. The total transmitted energy is numerically calculated and compared for waveguides with different slopes. The longer the tunnel length, the weaker the transmitted energy, which is in accordance with the tunnel effect explanation. Bibliography

References

[1] J. M. Arnold, L. B. Felsen: Coupled mode theory of intrinsic modes in a wedge. J. Acoust. Soc. Am. **79** (1986) 31–40.

[2] K. Motegi: Ultrasonics radiation into water by Lamb wave device using a piezoelectric ceramic plate with spatially varying thickness. Ultrasonics **37** (1999) 505–510.

[3] J. M. Arnold, L. B.Felsen: Intrinsic modes in a nonseparable ocean waveguide. J. Acoust. Soc. Am. **76** (1984) 850–860.

[4] V. Pagneux, A. Maurel: Located modes in acoustic wave guides with variable section. Proceedings in CD of 6th CFA, Lille, France, 8-11 April 2002.

[5] M. V. Perel, J. D. Kaplunov, G. A. Rogerson: An asymptotic theory for internal reflection in weakly inhomogeneous elastic waveguides. Wave Motion **41** (2005) 95–108.

[6] V. Pagneux, A. Maurel: Lamb wave propagation in elastic waveguides with variable thickness. Proc. Royal. Soc. A **462** (2006) 1315–1339.

[7] M. Ech-Cherif El-Kettani, F. Luppé, A. Guillet: Guided waves in a plate with linearly varying thickness: Experimental and numerical results. Ultrasonics **42** (2004) 807–812.

[8] Z. Hamitouche, M. Ech-Cherif El-Kettani, J.-L. Izbicki, H. Djelouah: Multi resonances of the S0 adiabatic mode propagating in a linearly varying cross section waveguide. IEEE Ultrasonics Symposium, New York, USA, 28-31 October 2007, P5E–7, 2303–2306.

[9] M. Ech-Cherif El-Kettani, P. Marical, M. V. Predoi: Experimental and numerical studies on lamb waves conversion in a waveguide with Gaussian section variation. IEEE Ultrasonics symposium, Vancouver, Canada, 3-6 October 2006, 5K–6, 1185–1188.

[10] P. Marical, M. Ech-Cherif El-Kettani, M. V. Predoi: Guided waves in an elastic plate with Gaussian section variation: Experimental and numerical resultsŤ. Ultrasonics **47** (2007) 1–9.

[11] Y. Cho, J. L. Rose: A boundary element solution for a mode conversion study of the edge reflection of Lamb waves. J. Acoust. Soc. Am. **99** (1996) 2097–2109.

[12] J. M. Galen, R. Abascal: Elastodynamic guided wave scattering in infinite plate. Int. J. Numer. Methods Eng. **58** (2003) 1091–1118.

[13] M. Koshiba, S. Karakida, S. M. Suzuki: Finite-element analysis of Lamb wave scattering in an elastic plate waveguide. IEEE Trans. Son. Ultrason **SU-311** (1984) 18–25.

[14] J. M. Galen, R. Abascal: Numerical simulation of Lamb wave scattering in semi-infinite plates. Int. J. Numer. Methods Eng. **53** (2002) 1145–1173.

[15] V. Pagneux, N. Amir, J. Kergomard: A study of wave propagation in varying cross-section waveguides by modal decomposition. Part I. Theory and validation. J. Acoust. Soc. Am. **100** (1996) 2034–2048.

[16] V. B. Galenko: On coupled modes theory of two-dimensional wave motion in elastic waveguides with slowly varying parameters in curvilinear orthogonal coordinates. J. Acoust. Soc. Am. **103** (1998) 1752–1720.

[17] J. Gao, J. Yang, L.-J. Cui, J.-C. Chang, M.-L. Qian: Modelling laser-generated guided waves in bonded plates by the finite element method. Ultrasonics **44** (2006) 985–989.

[18] B. Morvan, N. Wilkie-Chancelier, H. Duflo, A. Tinel, J. Duclos: Lamb wave reflection at the free edge of plate. J. Acoust. Soc. Am. **113** (2002) 1417–1425.

[19] A. Alippi, A. Bettucci, M. Germano: Anomalous propagation characteristics of evanescent waves. Ultrasonics **38** (2000) 817–820.